Corrigendum

Woods, A. H., Bonnecaze, R. T. and Zrubek, B. (2005). Oxygen and water flux across eggshells of *Manduca sexta. J. Exp. Biol.* **208**, 1297-1308.

In both the on-line and print versions of this paper, the left hand *y* axis of Fig. 6A was labelled incorrectly as:

Water vapour flux $\times 10^6$ (mol s^{-1} m^{-2}).

The correct label should read:

Water vapour flux $\times 10^5$ (mol s^{-1} m^{-2}).

The error does not affect any of the conclusions of the paper and the authors apologise for any inconvenience caused.

The Journal of Experimental Biology 208, 1297-1308
Published by The Company of Biologists 2005
doi:10.1242/jeb.01525

Oxygen and water flux across eggshells of *Manduca sexta*

H. Arthur Woods[1,*], Roger T. Bonnecaze[2] and Brandy Zrubek[1]

[1]*Section of Integrative Biology, The University of Texas at Austin, Austin, TX 78712, USA* and
[2]*Department of Chemical Engineering, The University of Texas at Austin, Austin, TX 78712, USA*

*Author for correspondence (e-mail: art.woods@mail.utexas.edu)

Accepted 28 January 2005

Summary

Insect eggs must obtain oxygen across the eggshell to support embryonic development. Because eggs are small, obtaining enough oxygen would seem trivial. Recent work, however, has shown that eggs of a moth, *Manduca sexta*, are oxygen limited at high but realistic temperatures (32–37°C) and that P_{O_2} drops steeply across the eggshell. Here we use theoretical and experimental approaches to partition the total resistance to oxygen flux among several steps in the oxygen cascade from environment to embryo. Standard mass-transfer analysis suggests that boundary layers of air around eggs, and around substrates to which they are attached, offer negligible resistance. Likewise, a mathematical model, parameterized using published and newly obtained morphological data, predicts that air-filled parts of the chorion also do not resist oxygen flux. This prediction was confirmed by experiments that measured rates of carbon dioxide emission from batches of eggs subjected simultaneously to hypoxia and inert gas substitution: depression of metabolic rate by hypoxia was not rescued when the diffusion coefficient of oxygen in air was doubled by substituting helium for nitrogen. The model did predict, however, that a set of subchoral layers (a crystalline chorionic layer, a wax layer and the vitelline membrane) could account for most or all of the total resistance to oxygen flux. Support for this prediction was obtained from two sequential experiments. First, eggs extracted with chloroform:methanol had highly elevated rates of water loss, suggesting that indeed eggs of *M. sexta* are waterproofed by wax. Second, rates of water loss and carbon dioxide emission from batches of eggs, measured from laying to hatching, changed in parallel over development. These data suggest that a single layer, likely a wax layer or a combination of wax and other subchoral layers, provides the main resistance to water efflux and oxygen influx.

Key words: eggshell, oxygen, water, tradeoff, inert gas substitution, chorion, wax, crystalline chorionic layer, oxygen limitation, mathematical model, moth, *Manduca sexta.*

Introduction

At oviposition, eggs of most insects contain all the materials and energy necessary for embryonic development, with the exception of oxygen. Obtaining oxygen would seem trivial; insect eggs are small and oxygen should diffuse rapidly from one point to another (Schmidt-Nielsen, 1984). Moreover, the literature on avian eggs would seem to support such a conclusion. Bird embryos also obtain oxygen by diffusion across an eggshell (Wangensteen and Rahn, 1970/1971). However, avian egg masses range from about 9 kg in the extinct *Aepyornus* down to 200–300 mg in some hummingbirds (Rahn and Ar, 1974), whereas insect eggs range from around 10 mg down to tens of μg (Hinton, 1981). Insect eggs therefore support much smaller volumes of metabolizing tissues with much higher surface-to-volume ratios; oxygen delivery should be easy.

Recently, Woods and Hill (2004) showed for eggs of a sphingid moth, *Manduca sexta*, that this is not so. Eggs developed more slowly in even moderate hypoxia (P_{O_2} 9–15 kPa) and did not survive extended exposure to P_{O_2} <9 kPa. Egg metabolic rates, measured as CO_2 emission, were depressed by hypoxia and stimulated by hyperoxia and the effect of P_{O_2} was stronger at higher temperatures. The work presented here asks: what is the identity and structure of the layer(s) resisting oxygen flux between environment and embryo? *A priori*, we suspect that the main resistance is associated with one or more layers of the eggshell, as these were the location of the steepest P_{O_2} gradient (Woods and Hill, 2004). To evaluate possible answers in a formal framework, we develop here a mathematical model of gas flux between embryo and environment. The model contains a series of resistances, each corresponding to one or more eggshell layers. With additional theory and a set of data on egg morphology and physiology, we derive quantitative estimates of the resistances – finding that most of it can be localized to one or a few layers beneath the chorion. The same layers also resist outward flux of water vapour, suggesting that these layers are the physical locus of an oxygen–water tradeoff.

Structure of insect eggs

The model focuses on eggshell layers common to most insect orders (Hinton, 1981; Margaritis, 1985), but with particular reference to eggs of Diptera (Margaritis et al., 1980) and Lepidoptera (Fehrenbach et al., 1987; Fehrenbach, 1995) and additional information specific to *M. sexta* (Dorn et al., 1987; Lamer and Dorn, 2001). One could, in such a model, include explicit terms describing each distinct eggshell layer – but there are too many (Fig. 1A) with poorly known properties. Our approach, therefore, is to collapse sets of layers into a few 'functional layers.' We do not model plastron respiration, but such a layer could easily be added following the work of Thorpe and Crisp (1947).

The outermost layer relevant to gas exchange is the boundary layer of air around the egg. The thickness of this layer depends on wind speed around the egg and on its oviposition substrate (e.g. leaf, stem, soil). We model mass transfer of oxygen through this layer with standard equations.

The outermost component of the eggshell itself is the chorion (Fig. 1A), which is composed primarily of protein. Chorion thickness varies among species from thin (<1 μm in *Drosophila*) to very thick (>40 μm in some saturniid moths; Margaritis, 1985). In *M. sexta*, the chorion is 7–8 μm thick (Orfanidou et al., 1992). Chorions of most species are penetrated by aeropyles: air-filled, hydrofuge tubes of radii ~1 μm, which are conduits for gases diffusing between embryo and environment (Hinton, 1981). At the base of the chorion, the aeropyles open into a thin trabecular layer (TL; Fig. 1A) – so-called because it is an interconnected series of vaulted chambers. This layer is thin (often <0.5 μm thick) and air-filled, and it extends over most or all of the surface area of the egg. Both chorion and trabecular layer are deposited by maternal follicular cells.

Beneath these layers are a crystalline chorionic layer (CCL), a wax layer and the vitelline envelope (VE; Fig. 1A). These layers constitute a set – they also are secreted by maternal follicular cells and are closely apposed (Margaritis et al., 1980). A CCL has been found in most of the insect species examined for it (eggs of *M. sexta* have not been examined) (Furneaux and Mackay, 1972; Margaritis et al., 1979; Margaritis and Mazzini, 1998; Papassideri et al., 2003). In *D. melanogaster*, the layer is ~40 nm thick (Papassideri and Margaritis, 1996) and in *Leptinotarsa decemlineata* it is ~1 μm thick (Papassideri et al., 2003). For most other species studied, CCL thickness lies between these extremes (Margaritis, 1985). The crystallized repeating units, likely proteins, exhibit a periodicity of about 10 nm in *D. melanogaster* (Papassideri et al., 2003) and similar spacing in other species (Margaritis, 1985). Papassideri and Margaritis (1996) suggesting that in *Drosophila* the layer controls water movement across the eggshell; if so, it could conceivably also affect oxygen flux. Unfortunately, no experimental data on CCL permeability to water or oxygen are available for any insect. Among the layers neglected in the model, the gas exchange properties of this one are potentially the most interesting.

Below the CCL is a thin wax layer (Fig. 1A). Waxes were first proposed as waterproofing agents in insect eggs over 50 years ago (Beament, 1946; Slifer, 1948) and have since been identified in a number of insect orders (Margaritis,

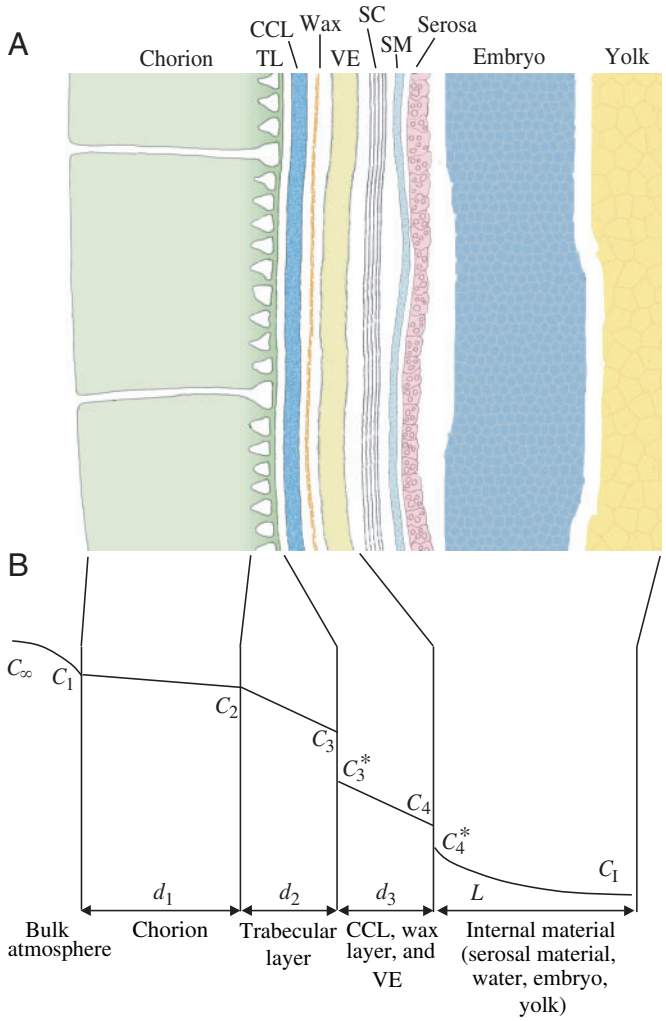

Fig. 1. (A) Schematic of an insect eggshell, drawn from published information on *Manduca* and *Drosophila*. Features are not to scale. From left to right, the layers are: chorion, trabecular layer (TL), crystalline chorionic layer (CCL), wax layer, vitelline envelope (VE), serosal cuticle (SC), serosal membrane (SM), serosa, embryo, yolk. From the VE outwards, all layers are in place at oviposition, having been secreted by maternal follicular cells. By contrast, the SC and SM are secreted from the serosa, which is derived from the blastoderm. The SC is secreted first, starting at about 12 h after oviposition (at 24°C), followed by the SM from 23–44 h after oviposition (Lamer and Dorn, 2001). The embryo develops closely apposed to the serosa (rather than deep within the yolk), both before and after katatrepsis. The yolk itself becomes cellularized in the first 12 h after oviposition (Lamer and Dorn, 2001). (B) Schematic of gas flux model. The model terms represent the characteristics of five different layers or sets of layers. From left to right they are: boundary layers around the egg or its substrate, chorion, trabecular layers, a combination of the CCL, wax layer and VE, and all remaining interior layers.

Table 1. *Definition of symbols and their values*

Symbol	Meaning	Units	Value
a	Measured equatorial axis of egg of *M. sexta*	m	7.84×10^{-4}
c	Measured polar axis of egg of *M. sexta*	m	6.84×10^{-4}
C_i	Concentration of oxygen at position i	mol m^{-3}	
C_∞	Concentration of oxygen in bulk atmosphere (at 25°C)	mol m^{-3}	8.583
D_{air}	Diffusion coefficient of oxygen in air	m^2 s^{-1}	2.09×10^{-5}
D_i	Diffusion coefficient in layer i	m^2 s^{-1}	
d_i	Thickness of layer i	m	
e	Ellipticity	None	0.489
H_i	Thermodynamic partition coefficient	None	
J	Flux of oxygen into an egg of *M. sexta*	mol s^{-1} m^{-2}	1.09×10^{-6}
k_E	External mass transfer coefficient	m s^{-1}	
k_I	Internal mass transfer coefficient	m s^{-1}	
k_m	Overall mass transfer coefficient	m s^{-1}	1.9×10^{-7}
K	Permeability coefficient	mol s^{-1} m^{-2} kPa^{-1}	
L	Characteristic length of leaf	m	0.1
l	Average distance between aeropyles	m	3×10^{-5}
R	Radius of an egg if it were perfectly spherical	m	7.5×10^{-4}
r	Radius of a single aeropyle	m	
S	Surface area of *Manduca* egg	m^2	7.07×10^{-6}
ν	Wind speed	m s^{-1}	
α	Fraction of chorion surface occupied by aeropyles	None	1.39×10^{-4}
β	Capacitance coefficient	mol m^{-3} kPa^{-1}	
ε	Fraction of trabecular layer that is air	None	0.7
υ	Kinematic viscosity of air	m^2 s^{-1}	1.6×10^{-5}
τ	Tortuosity of trabecular layer	None	4

1985), including Heteroptera, Diptera and Lepidoptera. Papassideri et al. (1991), in a detailed analysis of the structure of the wax in layer in *D. melanogaster*, showed that it was only ~5 nm thick and consisted of individual plaques of wax, each 0.5–1.0 μm in diameter, compressed between the overlying CCL and underlying VE (and possibly intercalated with them, Papassideri et al., 1991). Wax layers from non-drosophilids are poorly known, although they have been identified in a number of Lepidoptera (Telfer and Smith, 1970; Cruikshank, 1972; Salkeld, 1973; Barbier and Chauvin, 1974). Wax plates similar to those of *Drosophila* are seen in eggs of *Galleria mellonella* (Pyralidae) (Barbier and Chauvin, 1974). Each plate is ~10 nm thick and three or more plates may partially overlap. The total thickness of the wax layer appears to be <50 nm in most species. VE-associated waxes extracted from dechorionated eggs of six species of Diptera were composed primarily of *n*-alkanes and methyl-branched alkanes (Nelson and Leopold, 2003), similar in composition to the epicuticular waxes of pupae and adults. The wax layer in eggs of *M. sexta* has not been analyzed in comparable detail. Nelson and Sukkestad (1970) extracted total lipids from batches of *Manduca* eggs (59.5 μg egg^{-1}), from which a hydrocarbon fraction (3.1 μg egg^{-1}) was isolated. The hydrocarbons, which are thought to be VE-associated, were 50% *n*-alkanes (27- and 29-carbon) with the remainder primarily dimethylalkanes. Egg waxes likely also contain polar lipids of the kinds found by Buckner et al. (1984) in surface waxes of pupal *M. sexta*.

The VE (vitelline envelope) itself usually is thick (several μm) before oviposition (e.g. Salkeld, 1973), but it compresses afterwards and may be very thin (e.g. <0.5 μm, Barbier and Chauvin, 1977; Margaritis, 1985; Fehrenbach et al., 1987) by midway through development. Its permeability has not been measured but it is probably high, as brief extraction of *Drosophila* VE with wax-removing solvents (leaving the VE itself) renders the egg much more permeable to water (Schreuders et al., 1996). Biemont et al. (1981) suggest that eggs of the beetle *Acanthoscelides obtectus* are protected by a dense vitelline envelope, although they present no supporting experimental evidence. For model construction, we focus on the CCL, wax and VE layers as a functional unit (Fig. 1B), both because we have no way, practically, of manipulating them independently and because numerous authors have suggested that the layers may act as a single unit – e.g. that there is intercalation of wax into the VE (Margaritis, 1985) or that the crystalline layer organizes wax (Papassideri and Margaritis, 1996).

After oviposition, additional layers (serosal cuticle, serosal membrane, serosa, embryonic cuticle and tissue) develop or are secreted in a complicated spatiotemporal pattern beneath the VE. Excellent descriptions of these layers in *M. sexta* are given by Dorn et al. (1987), Lamer and Dorn (2001) and Berger-Twelbeck et al. (2003). Although one or more of these layers may be relevant to gas exchange, at present too little is known about them to afford more than guesses about their individual permeabilities. For simplicity, we model all of the subvitelline

layers as a single material (Fig. 1B). Finally, the characteristics of yolk may be important to gas exchange, although the bulk of yolk lies to the interior of the embryo. In *M. sexta*, yolk does become cellular (Lamer and Dorn, 2001) and presumably consumes oxygen.

Gas flux model

The first serious attempt to model oxygen flux into insect eggs was by Tuft (1950), who experimented with eggs of the bug *Rhodnius prolixus*. Eggs of this species obtain oxygen only through a set of pores (pseudomicropyles) located near the rim cap end of the egg. Using simple equations for the penetration of O_2 into tissues of different geometry, Tuft (1950) showed that eggs could obtain sufficient oxygen only if the trabecular layer was air-filled and extended over the whole egg surface under the chorion. Later, Hartley (1971) used detailed measurements of the chorion of eggs of a tettigoniid (*Homorocoryphus nitidulus vicinus*) to parameterize a flux model through the outer chorion. He concluded that water-filled, but not air-filled, parts of the chorion resist oxygen movement. Recently, Daniel and Smith (1994) developed equations describing the diffusive resistance of the single aeropyle in eggs of a bruchid beetle, *Callosobruchus maculatus*. None of the efforts to understand gas exchange by insect eggs approaches the sophistication and detail of efforts for bird eggs (see especially Wangensteen et al., 1970/1971; Wangensteen and Rahn, 1970/1971; Paganelli et al., 1975; Paganelli, 1980).

Our model is the first to consider individual layers explicitly. Consider a shell composed of three layers (Fig. 1B; Table 1), each with a diffusive resistance to mass-transfer of gas. The first two layers, the chorion and trabecular layer, contain air-filled pores of differing microstructure. The third, representing a composite of crystalline chorionic layer, wax and vitelline envelope, is considered to be a solid into which diffusing gas may dissolve. In addition, on the outside and inside of the layers described there may be additional resistance to mass-transfer – e.g. resistance by boundary layers of still air around the egg or from liquid between the bottom-most eggshell layer and the embryo. Note that at the interface between the second porous layer and adjoining third solid layer, there is a thermodynamic partitioning of the gases. Likewise, there is thermodynamic partitioning at the interface between the third, solid layer and the liquid interior of the egg. Throughout, our model refers to gas concentrations rather than partial pressures (see Appendix 1 in supplementary material, which shows how to convert between them).

If the thickness of each layer (d_i) is much less than the radius of curvature, R, we can neglect the effects of curvature and model the mass-transfer as occurring in one Cartesian direction (Fig. 1B; Hartley, 1971). At steady state, the flux J through each of the five regions (one external, three diffusive layers and one internal) is constant and is given by the expressions:

$$J = k_E (C_\infty - C_1), \quad J = \frac{D_1}{d_1}(C_1 - C_2), \quad J = \frac{D_2}{d_2}(C_2 - C_3),$$

$$J = \frac{D_3}{d_3}(C_3^* - C_4), \quad J = k_I (C_4^* - C_I), \qquad (1a–e)$$

where D_i is the diffusion coefficient of the gas in the ith layer of the shell, k_E and k_I are external and internal mass-transfer coefficients. The concentrations C_i of the diffusing species occur at the locations indicated in Fig. 1B. Asterisks indicate shifts in concentration due to thermal partitioning from one phase (e.g. air) into another (e.g. solid wax).

Assuming a linear thermodynamic relationship, $C_3=H_3C_3^*$ and $C_4=H_4C_4^*$, where H_3 and H_4 are constants (partition coefficients) and rearranging the terms above so the right-hand side involves only differences in concentration, one finds that:

$$\frac{J}{k_E} = C_\infty - C_1, \quad \frac{Jd_1}{D_1} = C_1 - C_2, \quad \frac{Jd_2}{D_2} = C_2 - C_3,$$

$$\frac{Jd_3H_3}{D_3} = C_3 - H_3C_4, \quad \frac{JH_3H_4}{k_I} = H_3C_4 - H_3H_4C_I. \qquad (2a–e)$$

Summing the last five equations cancels all concentrations except C_∞ and C_I, giving the following flux equation:

$$J = \left(\frac{1}{k_E} + \frac{d_1}{D_1} + \frac{d_2}{D_2} + \frac{d_3H_3}{D_3} + \frac{H_3H_4}{k_I}\right)^{-1} (C_\infty - H_3H_4C_I). \qquad (3)$$

Note that this expression can also be written as

$$J = k_m (C_\infty - H_3H_4C_I), \qquad (4)$$

where the overall mass-transfer coefficient is k_m is given by:

$$k_m = \left(\frac{1}{k_E} + \frac{d_1}{D_1} + \frac{d_2}{D_2} + \frac{d_3H_3}{D_3} + \frac{H_3H_4}{k_I}\right)^{-1}. \qquad (5)$$

Below, using both experiments and additional theory, we derive quantitative estimates for the resistance of each of the main eggshell layers to oxygen flux.

How large is a large resistance?

Equation 5 shows that the overall mass transfer coefficient k_m is the reciprocal of a sum of individual resistances, each corresponding to a different diffusion step. Evaluating whether individual resistances are large requires a benchmark for comparison. We therefore calculated the value of k_m that would depress the internal concentration of oxygen C_I to the values observed by Woods and Hill (2004). In particular, 3-day-old eggs at 24°C had minimum, central P_{O_2} levels of approximately 2 kPa as measured by an O_2 microelectrode, or about 10% of atmospheric P_{O_2} at sea level (~21 kPa). If we assume the egg's liquid contents are mostly water, then at air saturation the contents would contain 0.255 mol m^{-3} (Denny, 1993); thus, at 10% of saturation, C_I=0.0255 mol m^{-3}. Equation 4 can be rearranged to give:

$$k_m = \frac{J}{C_\infty - C_1 H_3 H_4}, \quad (6)$$

C_∞ is known and J can be calculated from data in Woods and Hill (2004), who found that the average 3-day-old egg (at 25°C, weighing 1.56 mg) emitted carbon dioxide at a rate of 6.5×10^{-12} mol s^{-1}. Assuming a respiratory quotient of 0.84 (Alleyne et al., 1997), it consumed O_2 at a rate of 7.7×10^{-12} mol s^{-1}. The surface area of an average egg is 7.07×10^{-6} m^2 (see Appendix 2 in supplementary material), so that the area-specific O_2 flux was 1.09×10^{-6} mol s^{-1} m^{-2}. We have no direct measures of H_3 or H_4, but estimate them as 10 and 3, respectively (Battino et al., 1983). Thus, the internal concentration of O_2 will be 10% of saturation if k_m=1.16×10^{-6} m s^{-1} and the overall resistance, $1/k_m$, is 8.57×10^5 s m^{-1}. This value provides a benchmark for evaluating resistances of individual layers.

Material and methods

Animals

Eggs were derived from a laboratory colony of *Manduca sexta* L. All stages were exposed to a 14 h:10 h L:D photoperiod. Eggs, larvae and pupae were kept at 25°C and adults at 24°C. Adults were given 30% honey water and potted tobacco plants for oviposition. To facilitate egg collection, the adult scotophase was set to begin at 07:00 h.

Microscopy

Both light and electron microscopy were used to measure aeropyle density and cross-sectional area. Density was measured on 10 isolated chorions washed gently in saline to remove yolk and other debris. Cleaned chorions were mounted under oil and visualized with a Zeiss Axioplan2 compound microscope fitted with an ocular micrometer grid (400× magnification, at which the grid was 250 μm on a side, or 62,500 μm^2 total). On each chorion the grid was positioned randomly over 5–7 locations and the number of aeropyles within the grid was counted.

For scanning electron microscopy (SEM), fresh chorions were washed in saline and fixed overnight in 2% glutaraldehyde in sodium cacodylate buffer (200 mmol l^{-1}, pH 7.4, 4°C). Subsequently, they were rinsed, dehydrated in an ethanol series and stored over desiccant at room temperature. Samples were then sputter-coated with gold, mounted and viewed (Hitachi S-4500 Field Emission SEM, 5 kV). On each of five eggs, 10 randomly picked aeropyles were photographed and two orthogonal diameters on each aeropyle image were measured using image analysis software (Scion Image v. beta 4.0.2, Scion Corporation, Frederick, MD, USA), from which cross-sectional areas could be calculated using the equation for the area of an ellipse.

Inert gas substitution

The diffusion coefficient of gaseous O_2 in a binary mixture depends on the molecular mass of the other gas. Air, for example, consists essentially of O_2 and N_2 and the diffusion coefficient of O_2 in air, D_{air}, is 2.09×10^{-5} m^2 s^{-1}. If N_2 (molecular mass 28) is replaced entirely by He (molecular mass 4) of the same partial pressure, D_{air} rises 2.2-fold to

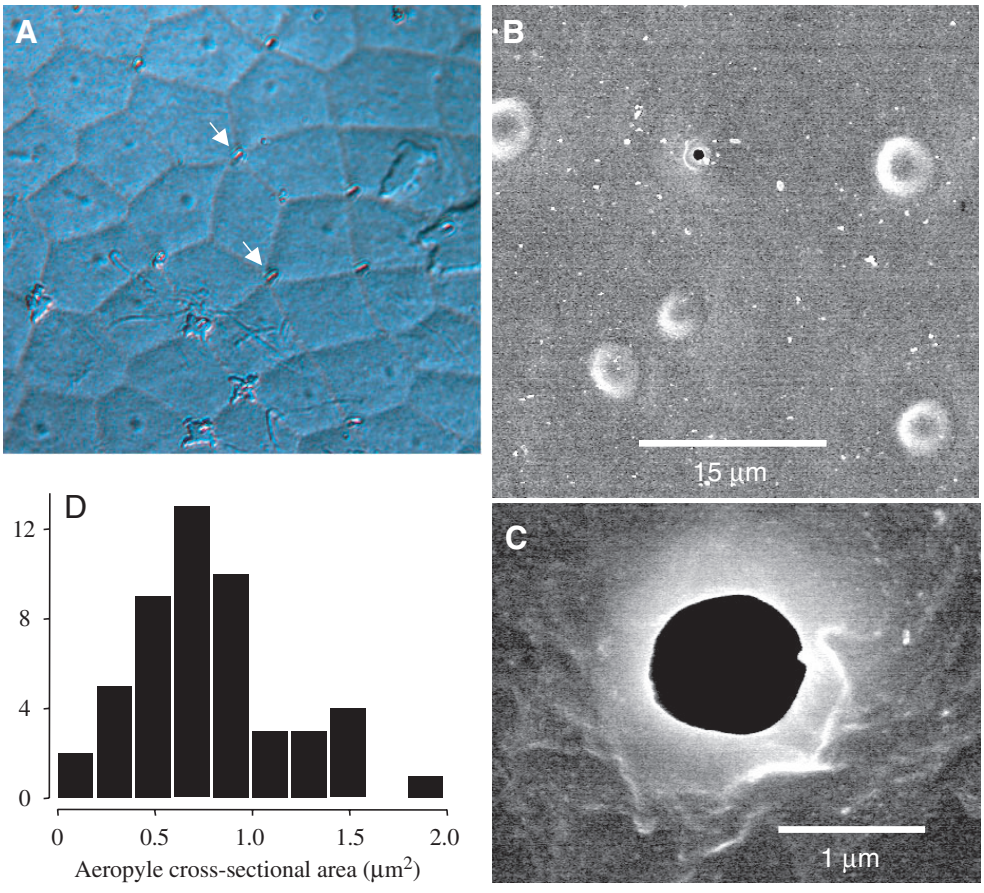

Fig. 2. Aeropyle density and cross-sectional area of eggs of *Manduca sexta*. (A) Light microscope view (400×, immersed in oil) of the surface of a chorion removed from the egg and washed in saline. Polygons are the imprints of the follicular cells that deposited the chorion (Orfanidou et al., 1992). White arrows point to two aeropyles; about 13 aeropyles are visible in this field. (B) SEM view of the outer surface of a chorion. Polygons are not visible, but dimples (see A) are. A single aeropyle is in the upper left quadrant. (C) Close up view of a single aeropyle. (D) Histogram of aeroyple cross-sectional areas. Data represent 10 aeropyles from each of five eggs (N=50). Mean cross-sectional area (±S.E.M.) is 0.775 ± 0.054 μm^2.

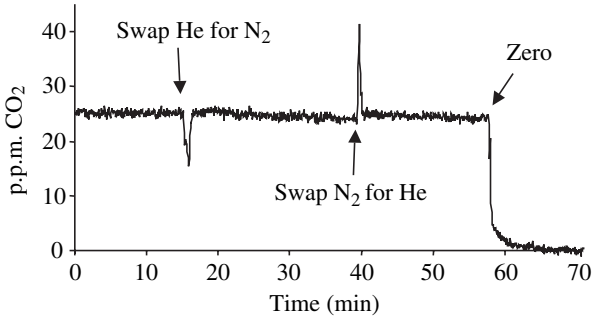

Fig. 3. Control trace demonstrating successful identification of a thermal conversion factor for switching between N_2 and He using a single mass-flow controller. The stream flowing through the CO_2 analyzer was composed of 5 ml min^{-1} of a span gas (505 p.p.m. CO_2 in N_2), 21 ml min^{-1} O_2 and 74 ml min^{-1} of either He or N_2 carrier. Using the identified conversion factor (1.37), we were able to switch between carrier gases without affecting the reading from the CO_2 analyzer (~25 p.p.m. CO_2, which is 5% of 505 p.p.m.).

4.60×10^{-5} m^2 s^{-1}. Importantly, substitution of He for N_2 does not affect the diffusion of O_2 in liquids (e.g. water, yolk) or solids (e.g. wax). Therefore, if the chorion and trabecular layers really do not resist flux, then substituting He for N_2 should not rescue O_2-starved eggs.

We tested this prediction by measuring metabolic rates while simultaneously manipulating O_2 content and the inert carrier identity of gas mixtures supplied to batches of eggs. Metabolic rate was measured as CO_2 emission using flow-through respirometry. Batches of eggs (*M. sexta*) that were either 1.5 or 3 days old and weighing between 330 and 690 mg (approximately 210–450 eggs per batch) were placed into a glass chamber (large enough so that the eggs were in a monolayer) and submerged in a temperature-controlled water bath set to a temperature (37°C) that we knew from previous work (Woods and Hill, 2004) gave maximal metabolic rates. To ensure that incoming air was thermally equilibrated, gas upstream of the chamber was first directed through 0.5 m of coiled, submerged, $\frac{1}{4}$-inch copper tubing. Gases were mixed from cylinders of pure O_2, N_2 and He using calibrated mass flow controllers (2 Tylan FC-2900, Torrance, CA and UNIT UFC-1100, Yorba Linda, CA, USA) and mixing electronics (MFC-4, Sable Systems, Las Vegas, NV, USA). The gas stream (100 ml STPD min^{-1}) was directed past the eggs, through a small volume of indicating Drierite to remove water vapour and into a carbon dioxide analyzer (CA-2A, Sable Systems), which was calibrated frequently with pure N_2 (zero) and 505 p.p.m. CO_2 in N_2 (span, Airgas, Radnor, PA, USA). Data were logged using Datacan V software (V5.4, Sable systems) receiving digital signals from an A/D converter (UI2, Sable Systems), which itself received analog signals from the instruments. In addition to CO_2, we logged temperature in a separate chamber otherwise identical to the experimental chamber but fitted with a T-type thermocouple (connected to a TC-1000 thermocouple meter, Sable Systems).

Because flows of N_2 and He were both controlled by the same mass flow controller (factory-calibrated for N_2 flow), we

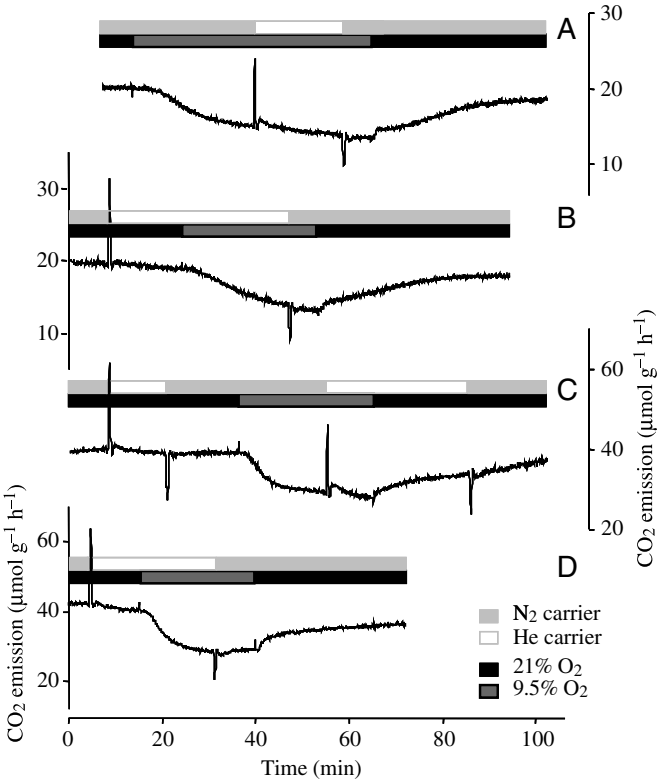

Fig. 4. CO_2 emission (at 37°C) by batches of *Manduca sexta* eggs either 1.5 d (A and B) or 3 day old (C and D). Each batch contained 210–450 eggs. Eggs were exposed, in series, to either 21 or 9.5% O_2 with either He or N_2 making up the balance. Only variation in O_2 availability affected metabolic rates; swapping carrier gases (which altered the diffusion coefficient of O_2 in the air filled parts of the chorion and trabecular layer) had no effect.

first needed to determine the appropriate thermal conversion factor. To do so, we generated a gas stream consisting of (all gas volumes STPD) 5 ml min^{-1} span gas (505 p.p.m. CO_2 in N_2 controlled by a calibrated mass flow controller), 21 ml min^{-1} O_2 and 74 ml min^{-1} N_2 or He (through the same controller). By switching repeatedly between N_2 and He, we empirically identified a thermal conversion factor (1.37) that, in our system, gave identical readings from the CO_2 analyzer (~25 p.p.m. CO_2, which is 5% of 505 p.p.m.).

Once the conversion factor was determined, we measured rates of CO_2 emission of batches of eggs that experienced, in series over 1–2 h, all four combinations of the following conditions: 21% O_2 in N_2, 21% O_2 in He, 9.5% O_2 in N_2 and 9.5% O_2 in He.

Rates of water loss before and after solvent extraction

The three layers underneath the trabecular layer – a crystalline layer, a wax layer and the vitelline envelope – are represented together in the model by the term d_3H_3/D_3. Below we focus on the wax layer, primarily because experimental manipulations are feasible. However, the crystalline chorionic layer itself probably plays a role in controlling the diffusion of

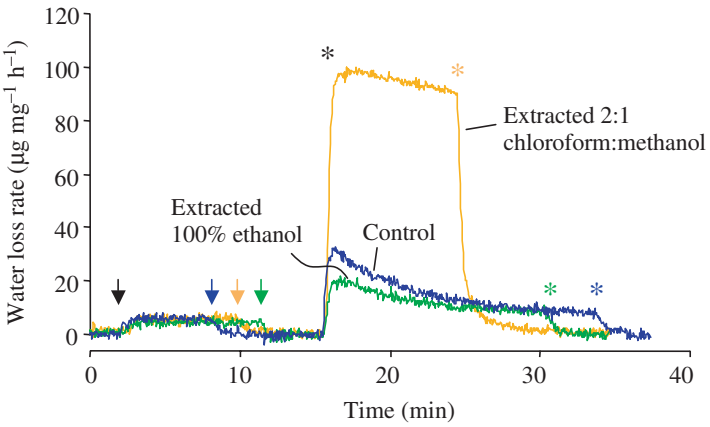

Fig. 5. Water loss (at 25°C) from batches of 2 day old *Manduca sexta* eggs. Each batch contained 40 eggs. The first few minutes of each trace represent a baseline reading (air stream directed through an empty chamber). Air streams were then redirected through the egg-containing chamber (black arrow) followed by another baseline reading (colored arrows). During the second baseline, batches were extracted for 1 min in 100% ethanol or 2:1 (v:v) chloform:methanol, blotted dry and returned to their chambers. A control batch was not extracted. The air stream was then directed again through the egg-containing chamber (black asterisk), after which a final baseline reading (colored asterisks) was taken.

gases, as suggested by Papassideri and Margaritis (1996). The role of the vitelline envelope in gas flux is unknown.

Batches of 40 2-day-old eggs were placed into a water-jacketed, stainless-steel chamber (custom built) designed to interface with a gas multiplexer (TR-RM8, Sable Systems) (see Woods and Hill, 2004 for details). The chamber temperature was maintained at 25°C by a recirculating water bath. An air stream (50 ml min^{-1}, dry, 21% O_2, mixed from cylinders of pure O_2 and N_2) was directed through the egg chamber, then past a thin-film capacitance humidity sensor (RH-100, Sable Systems) which had been calibrated with dry air (zero) and an air stream humidified to 2.336 kPa water vapour pressure (span; humidified by bubbling the stream through a flask of water held at 20°C).

To remove water vapour adhering to the egg surface, eggs were left in the chamber for ~30 min prior to measurement. Subsequently, a baseline reading was taken (through an empty chamber) and the air stream flowing past the eggs was sampled for ~5 min. This reading allowed calculation of the rate of water loss of unmanipulated eggs. During the subsequent baselining, the batch of eggs was removed from the water-jacketed chamber and extracted (room temperature) for 1 min with either chloroform:methanol (2:1 v:v; a general solvent for lipid extraction) or 100% ethanol (polar solvent), blotted briefly and returned to the chamber. After 2 min of flushing, the air stream was sampled again. A control batch was manipulated identically except that it was not exposed to solvent.

Developmental changes in metabolism and water loss

Data on artificial wax membranes indicate that wax permeability to O_2 may be very low (Donhowe and Fennema, 1993). These data suggest that the wax layer in insect eggshells may resist both water and oxygen flux. If metabolic demand for O_2 increases over development (which preliminary experiments showed was the case), embryos may thin or alter the wax layer to enhance O_2 delivery; if so, eggs should also lose water at higher rates towards the end of incubation. We tested this prediction by measuring metabolic rate (as CO_2 emission) while also measuring water loss rate over most of the period from laying to hatching.

Eggs of known synchronized age were obtained by introducing a potted tobacco plant into the adult mating cage for 2 h. Eggs were stripped from leaves, sorted randomly into three batches of 40, weighed and placed into water-jacketed (27°C) respirometry chambers within 6 h (maximum egg age 8 h). The flow-through system consisted of (calibrated) water vapour and CO_2 analyzers described above connected in series, with a small Drierite column between them. The air stream (dry, normoxic; 50 ml min^{-1} STPD) was directed sequentially, *via* computer control of a gas multiplexer, through each of the sample chambers and a blank (baseline) chamber. Each chamber was sampled for 30 min, during which time the other three chambers were flushed continuously (50 ml min^{-1} per chamber).

Results

External resistance to flux, 1/k_E

Boundary layers of air around eggs, or around the leaves to which they are attached, may retard O_2 transfer enough to produce significant gradients. To evaluate this possibility, we model two physical situations – a free, spherical egg (not attached to any surface) and an egg attached to a flat plane (many insects, including *M. sexta*, attach eggs to leaves).

The equation for forced convection around a solid sphere (Cussler, 1997, p. 227) is given by:

$$\frac{k_E R}{D_{air}} = 1 + 0.3\left(\frac{2R\nu}{\upsilon}\right)^{\frac{1}{2}}\left(\frac{\upsilon}{D_{air}}\right)^{\frac{1}{3}}, \quad (7)$$

where ν is bulk wind speed and υ is kinematic viscosity or air. Rearranging to solve for k_E gives:

$$k_E = \frac{D_{air}}{R}\left[1 + 0.3\left(\frac{2R\nu}{\upsilon}\right)^{\frac{1}{2}}\left(\frac{\upsilon}{D_{air}}\right)^{\frac{1}{3}}\right]. \quad (8)$$

When there is no convection (i.e., no wind), this expression reduces to:

$$k_E = \frac{D_{air}}{R}, \quad (9)$$

which gives the minimum mass transfer coefficient

(0.0279 m s^{-1}) under calm conditions (a maximum resistance of 35.9 s m^{-1}). With convection the resistance is lower still.

It may be more realistic to model eggs attached to a leaf. The equation for laminar flow across a plate of length L (Cussler, 1997, p. 227) is:

$$\frac{k_E L}{D_{air}} = 0.646 \left(\frac{L\nu}{\upsilon}\right)^{\frac{1}{2}} \left(\frac{\upsilon}{D_{air}}\right)^{\frac{1}{3}} . \quad (10)$$

Solving for k_E and assuming a leaf length of 0.1 m, we find that k_E is only about 10-fold lower than for forced convection around a sphere. Thus, neither assumed geometry nor wind speed gives a resistance more than 0.1% of the value calculated above.

Resistance of the chorion

In eggs of *M. sexta*, the chorion is ~7 μm thick (d_1=7×10^{-6} m) (Orfanidou et al., 1992). If aeropyles have the same diameter (the diameter at the chorion's outer surface) for their entire length, the effective diffusion coefficient in the chorion is:

$$D_1 = \alpha D_{air} , \quad (11)$$

where is the fraction of the chorion surface area occupied by aeropyles. The average surface area of eggs from our colony, 7.07×10^{-6} m^2, can be calculated directly from measures of egg shape (see Appendix 2 in Supplementary material).

Aeropyle density appeared not to vary with location on the eggshell. On average we counted 15.08 aeropyles per grid, giving an overall aeropyle density of 2.41×10^8 aeropyles per m^2. The average egg thus contains 1703 aeropyles (=2.41×10^8 aeropyles m^{-2} ×7.07×10^{-6} m^{-2}). This value is lower than Ofanidou et al. (1992) suggested. They observed aeropyles (p. 738) "at periodic distances of approximately 30 μm", equivalent to ~1.6×10^9 aeropyles m^{-2} or about 10,000 aeropyles per egg. The cause of the discrepancy is unclear; we show below, however, that variation in aeropyle number between the two values has a negligible effect on resistance to gas flux.

Aeropyles were obvious at a number of scales (Fig. 2B,C). They appeared almost perfectly round and few (14%) were obstructed by any visible material. The average area of an aeropyle (±S.E.M.) was 0.755±0.054 μm^2, in good agreement with Orfanidou et al. (1992), who visualized aeropyles of ~1.5 μm in diameter (1.76 μm^2). Together with the estimated total number of aeropyles, we calculate that the average egg has approximately 984 μm^2 (9.84×10^{-10} m^2) of aeropyle cross-sectional area. The fraction of total area occupied by aeropyles (α), therefore, is 0.000139. D_1 is thus 2.91×10^{-9} m^2 s^{-1} and the resistance of the chorion, d_1/D_1 is 2409 s m^{-1}. Higher numbers of aeropyles would be give even lower resistances. The value is larger than the external resistance of boundary layers but still is less than 0.3% of the benchmark resistance (8.6×10^5 s m^{-1}).

An objection is that we assumed aeropyles of uniform radius (cylinders), whereas they may actually taper as they approach the inner surface of the chorion (as in e.g. the moth *Antheraea polyphemus*, Margaritis and Mazzini, 1998). The consequences of this shape for gas diffusion have been explored for bird eggshells by Tøien et al. (1987, 1988), with the general conclusion that the narrow, inner portion of the funnel accounts disproportionately for the overall resistance. In eggs of *M. sexta*, this effect may be important. However, if the aeropyle radius at the inner chorion were even threefold smaller, the resistance would still be small. An upper bound can be estimated by assuming that the entire radius was threefold less – in this case, the overall resistance to flux would be ninefold higher, or 2.2×10^4 s m^{-1}. This value still only represents about 2.5% of the benchmark resistance.

Resistance of the trabecular layer

A priori, the thin trabecular layer (d_2=0.3 μm, or 3×10^{-7} m; Orfanidou et al., 1992) would seem not to provide much resistance – but it is worth a brief calculation nonetheless. The diffusion coefficient of O_2 in the trabecular space can be estimated as:

$$D_2 = \frac{\varepsilon D_{air}}{\tau} , \quad (12)$$

where ε is the fraction of the trabecular space that is air and τ is its tortuosity. The photographs of *M. sexta* eggs in Orfanidou et al. (1992) suggest that ε is greater than 0.5. τ is unknown, but most for most complex, porous solids, such as the trabecular layer, it is between 2 and 6 (Cusser, 1997, p. 173). Assuming ε=0.7 and τ=4, we estimate that D_2= 3.66×10^{-6} m^2 s^{-1} and therefore that trabecular resistance, d_2/D_2=0.082 s m^{-1}. The distance between pillars (h) in the trabecular layer is small enough (0.1–0.2 μm) that it approaches the mean free path of O_2 in air (λ=0.067 μm at room temperature). The kinetics of the diffusion process therefore lie near a transition point between Fickian and Knudsen regimes (Cussler, 1997). In Knudsen diffusion, molecules of O_2 collide more often with walls than with other gas molecules. Here we ignore these effects, because Knudsen diffusion predominates only when h<<λ.

Inert gas substitution

Because flows of both N_2 and He were controlled by the same mass flow controller, we first empirically determined an appropriate thermal conversion factor (1.37). A typical control trace using this factor is shown in Fig. 3.

As shown in Fig. 4, only variation in O_2 content affected metabolic rates. Swapping He for N_2 did not rescue the depressed metabolic rates of eggs in hypoxia; nor did swapping N_2 for He further depress metabolic rates of eggs already in hypoxia. This result did not depend on egg age.

Resistance of subchoral layers

Prior to extraction with organic solvents, all three batches of eggs had similarly low rates of water loss (Fig. 5; 4–6 μg mg^{-1} h^{-1}, comparable to values measured

gravimetrically by Woods and Singer, 2001). After extraction, water loss from the batch exposed to chloroform:methanol rose 18-fold to 90 μg mg^{-1} h^{-1}. Control eggs and those extracted in 100% ethanol had rates of water loss that rose 4–6-fold before falling back to values only slightly above pre-extraction values. The initial rise likely represents water vapour that had adhered to the outer chorion during the eggs' brief removal from the chamber. The pattern of solvent effects is consistent with Slifer's (1948) solubility data on waxes extracted from eggshells of a grasshopper, *Melanoplus differentialis*, which she found to be soluble in chloroform but not alcohol.

Developmental changes in metabolism and water loss

In the first 40 h of development, rates of metabolism and water loss rates both were low (Fig. 6A). Thereafter, metabolic rates rose more-or-less continuously to the end of development; rates of water loss followed a similar trajectory.

These correlative data indicate that the layer or layers responsible for waterproofing the egg – probably wax – likely also resist the flux of metabolic gases. A more quantitative analysis is possible. Wax permeability to water vapour can be calculated under the following assumptions: (1) that the wax layer accounts for all of the resistance to water vapour in the eggshell; (2) that the vapour pressure gradient across the eggshell is 3.56 kPa (from saturation at 27°C to zero); (3) and that wax layer thickness is 50 nm (d_3). If, like beeswax, eggshell waxes have an O_2:water vapour permeability ratio of 1.49% (Donhowe and Fennema, 1993), the permeability to O_2 (K) can then be calculated from water vapour permeabilities (averaged across the three batches). We then calculated the magnitude of the P_{O_2} gradient across the wax layer using the equation $\Delta P_{O_2}=Jd_3/K$, assuming that O_2 influx (J) is CO_2/0.84 emission. These calculations indicate (Fig. 6B, solid line) that increasing permeability of the wax over development (shown by rising rates of water loss) largely offsets increasing metabolic demand – consequently, the P_{O_2} gradient stays near 10 kPa. Given the number assumptions underlying these values, they match up remarkably well with the ΔP_{O_2} observed by Woods and Hill (2004) of 10–15 kPa in the first 100 μm across the eggshell. Likewise, values for permeability, corresponding to resistances of 10^5–10^6 s m^{-1}, match up well with the benchmark resistance. Additional calculations, using only a constant permeability (equivalent to that calculated at 32 h, a point of low permeability), show (Fig. 6B, dotted line) that eggshell permeability must increase if rising metabolic demand is not to create an impossibly large ΔP_{O_2}.

Internal resistance to flux, H_3H_4/k_I

The resistance of layers beneath the vitelline envelope depends on the permeability of the serosal cuticle and the geometry, location and permeability of the embryo. One estimate of the mass transfer coefficient, k_I, is D_{H_2O}/L, where L is the distance from the eggshell to the embryo. *M. sexta* develop just under the chorion, wrapped around yolk to the interior (Dorn et al., 1987). Assuming a distance between eggshell layers and embryo of 75 μm and that the diffusion

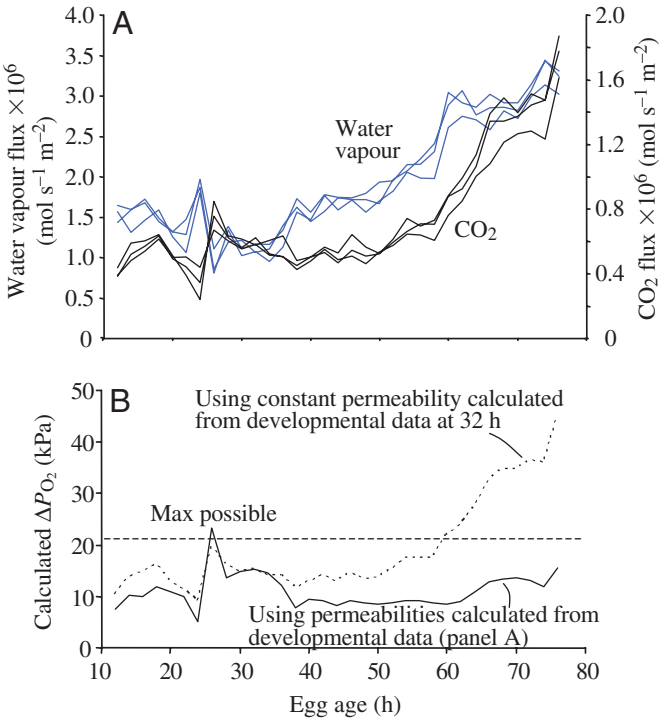

Fig. 6. (A) CO_2 (black) and water vapour emission (blue) by three batches of eggs from laying to hatching (27°C). Each batch contained 40 eggs. (B) Calculated drop in P_{O_2} (in kPa) across the wax layer using permeabilities calculated from developmental data in panel A (solid) or and from assuming a constant permeability equivalent that calculated for eggs of age 32 h (see text for details). Because P_{O_2} at sea level is approximately 21 kPa, this value sets the upper bound on possible ΔP_{O_2}.

coefficient of O_2 in the intervening material is the same as its value in water (2.38×10^{-9} m^2 s^{-1} at 25°C; Denny, 1993), $k_I=3.17\times10^{-5}$ m^1 s^{-1} and the fifth resistance term, H_3H_4/k_I, is 9.5×10^5 s^{-1} m^{-1}, about 20% of the benchmark value. This value surely changes as serosal and larval cuticles form. Oxygen transport to the egg's center is even more difficult. If we set L to the egg's radius (~0.75 mm, or 0.00075 m), then H_3H_4/k_I 9.5×10^6 s^{-1} m^{-1}. This value is more than 100% of the calculated benchmark, indicating that diffusive O_2 supply to central regions may be inadequate – although the metabolic density of yolk likely is much lower than of embryonic tissues. A detailed analysis of flux into the embryo and yolk will be forthcoming.

Discussion

The literature on insect eggshells is replete with suggestions that chorion morphology reflects the constraints of diffusive gas exchange (e.g. Chauvin and Barbier, 1972; Hinton, 1981; Margaritis, 1985; Papanikolaou et al., 1986; Daniel and Smith, 1994). It may well do so in species whose eggs lack aeropyles (e.g. *A. obtectus*; Biemont et al., 1981) or in species obtaining O_2 through unusual structures, such as respiratory appendages (e.g. *Drosophila*). Our parameterized model, however, predicts

that the air-filled chorion and trabecular layer of *M. sexta* do not provide any significant resistance to O_2 flux, or to water vapour flux in the opposite direction. We tested this prediction directly using inert gas substitution (Dudley and Chai, 1996). This technique has been used by Paganelli et al. (1975) to examine diffusion of gases across eggshells of hens (*Gallus domesticus*) and by Birchard (2000) in a study of gas exchange by pupae of *Hylaphora cecropia* (Lepidoptera, Saturniidae). The prediction was confirmed – doubling the diffusion coefficient of O_2 in the chorionic and trabecular spaces by substituting He for N_2 did not rescue eggs whose metabolic rates had been depressed by an approximate twofold decrease in ambient O_2 availability. Most published estimates of aeropyle diameter, number and length for different species do not differ by more than an order of magnitude from our data on *M. sexta*, suggesting that for terrestrial eggs the chorion's irrelevance to gas exchange is general.

A recent claim to the contrary (Daniel and Smith, 1994) in fact supports this conclusion. The authors found that the size and shape of the single aeropyle in eggs of the beetle *Callosobruchus maculatus* was correlated with metabolic rate between strains – eggs from a Yemeni strain had both higher metabolic rates (2×) and shorter, wider aeropyles than a Brazilian strain. The authors argued that shorter, wider aeropyles are an adaptation to enhance O_2 flux. However, the drop in O_2 concentration from the top to the bottom of the aeropyle is insignificant regardless of strain. Using the Fick equation and values for rate of oxygen consumption and aeropyle morphology from Daniel and Smith (1994), it is straightforward to show that if the Yemeni strain had aeropyles of Brazilian dimensions, the $[O_2]$ at the bottom of the aeropyle would have been ~8.37 mol m^{-3}. For comparison, air at 30°C (their test temperature) has a $[O_2]$ of 8.43 mol m^{-3} (Denny, 1993).

Previous work on *M. sexta* in our laboratory (Woods and Hill, 2004) showed that the P_{O_2} gradient across the eggshell is very steep, though the measurement resolution was not fine enough to detect gradients across individual layers. With the chorion and trabecular layers eliminated as candidates, the resistance must lie in one or more subchoral layers. Two observations implicate a wax layer specifically. First, extraction of eggs with chloroform:methanol (which extracts a broad range of lipids) led to markedly higher rates of water loss, suggesting that eggs of *M. sexta* are indeed waterproofed by wax. This conclusion does not exclude a role for the crystalline chorionic layer, which may also be destroyed by organic solvents. Second, from laying to hatching, rates of metabolism and water loss were strongly correlated. It appears that as metabolic rate increases embryos obtain adequate O_2 only by increasing the conductance of one or more layers, leading to higher rates of water loss. See Schmidt-Nielsen (1984) for a discussion of this tradeoff in bird eggs.

What remains is to develop a mechanistic view of how an oxygen–water tradeoff is manifest in subchoral layers. Previous work on waxes suggests the problem will not be trivial – even the problem of waterproofing alone has been controversial (Lockey, 1988). Beament (1945, 1961, 1968) championed the idea that resistance to water flux through thin wax layers stems not from the properties bulk wax but from a single monolayer of polar lipid molecules interacting with and organized by a substrate, i.e. the cuticle. The monolayer hypothesis, however, has since been criticized on a number of fronts (Gilby and Cox, 1963; Lockey, 1976; Toolson et al., 1979; Machin, 1980). More recent work (Gibbs, 1998, 2002) has focused on the effects of lipid chain length and structure on phase transitions, finding that phase behaviour is a major factor influencing cuticular permeability. These latter results suggest that bulk properties of wax layers, rather than interaction with a substrate, determine their permeability to water. Complications in this model arise from the behaviour of 'bulk waxes' – which if they contain many different lipid species can exist in multiple alternative packing arrangements or as separate, coexisting solid and liquid phases (Gibbs, 1998). How O_2 moves across such heterogeneous material is of particular interest.

In insect eggshells specifically, interactions between waxes and the crystalline chorionic layer may also occur (Margaritis et al., 1980). Major structural units in the crystalline layer are arranged periodically at intervals of 8–10 nm and smaller units at 3.5–5.5 nm (Margaritis, 1985); the open distances between units appear to be as low as 1 or 2 nm (Margaritis et al., 1984; Margaritis and Mazzini, 1998). The scale of these features is of the same order as the physical dimensions of individual wax molecules. For comparison, a straight-chain alkane containing n carbon atoms has a length of $(n–1)*1.27$ Å (1 nm=10 Å) between terminal carbons (Ocko et al., 1997). Thus a C-27 alkane would have a length of about 33 Å (3.3 nm), long enough to bridge spaces within the crystal lattice. It would also be narrow enough to intercalate into the crystal. Alternatively, polar lipids could be organized by interaction with polar sites on the surface of the crystalline layer (*à la* Beament). A still more radical hypothesis is that the crystalline layer itself is responsible for most of the waterproofing *and* most of the resistance to O_2 flux. Evaluating this last idea will require more detailed information, presently unavailable, on the sequences and arrangement of crystalline proteins.

Our work has both ecological and evolutionary implications. First, the wax layer and possibly also the vitelline envelope and crystalline chorionic layers, are the physical locus of a tradeoff between oxygen influx and water vapour efflux. Studies examining the physiological ecology of insect eggs (i.e. relationships among geographic distributions, eggshell structure, desiccation resistance and temperature-associated oxygen shortage) should focus explicitly on these subchoral layers. Second, the division of labor among eggshell layers – the chorion functioning to protect subchoral layers and embryo from mechanical threats (Hinton, 1981) and the subchoral layers controlling the fluxes of water, oxygen and carbon dioxide – indicates that the two sets of layers may be functionally and genetically decoupled over evolutionary time and likely are shaped by distinct sets of selection pressures.

We thank John Mendenhall, Michael Schmerling and the Texas Materials Institute (University of Texas at Austin) for SEM support and Dave Parichy for access to a compound light microscope. Two anonymous reviewers provided comments that substantially clarified the work. This work was supported by The University of Texas at Austin and a grant from the National Science Foundation to H.A.W. (IBN-0213087).

References

Alleyne, M., Chappell, M. A., Gelman, D. B. and Beckage, N. E. (1997). Effects of parasitism by the braconid wasp *Cotesia congregata* on metabolic rate in host larvae of the tobacco hornworm *Manduca sexta*. *J. Insect Physiol.* **43**, 143-154.

Barbier, R. and Chauvin, G. (1974). Ultrastructure et rôle des aéropyles et des enveloppes de l'oeuf de *Galleria mellonella*. *J. Insect Physiol*. **20**, 809-820.

Barbier, R. and Chauvin, G. (1977). Déterminisme de la transformation de l'enveloppe vitelline des oeufs de Lépidoptères. *Inter. J. Insect Morphol. Embryol*. **6**, 171-179.

Battino, R., Rettich, T. R. and Tominaga, T. (1983). The solubility of oxygen and ozone in liquids. *J. Phys. Chem. Ref. Data*, **12**, 163-178.

Beament, J. W. L. (1945). The cuticular lipoids of insects. *J. Exp. Biol.* **21**, 115-131.

Beament, J. W. L. (1946). The waterproofing process in eggs of *Rhodnius prolixus* Stähl. *Proc. Roy. Soc. Lond. B* **133**, 407-418.

Beament, J. W. L. (1961). The water relations of insect cuticle. *Biol. Rev.* **36**, 281-320.

Beament, J. W. L. (1968). Lipid layers and membrane models. In *Insects and Physiology* (ed. J. W. L. Beament and J. E. Treherne). New York: American Elsevier Publishing Company.

Berger-Twelbeck, P., Hofmeister, P., Emmling, S. and Dorn, A. (2003). Ovicide-induced serosa degeneration and its impact on embryonic development in *Manduca sexta* (Insecta: Lepidoptera). *Tissue Cell* **35**, 101-112.

Biemont, J. C., Chauvin, G. and Hamon, C. (1981). Ultrastructure and resistance to water loss in eggs of *Acanthoscelides obtectus* Say (Coleoptera: Bruchidae). *J. Insect Physiol.* **1981**, 667-679.

Birchard, G. F. (2000). The effect of changing the gaseous diffusion coefficient on the mass loss pattern of *Hyalophora cecropia* pupae. *Physiol. Biochem. Zool.* **73**, 488-493.

Buckner, J. S., Nelson, D. R., Fatland, C., Hakk, H. and Pomonis, J. G. (1984). Novel surface lipids of diapausing *Manduca sexta* pupae. *J. Biol. Chem.* **259**, 8461-8470.

Chauvin, G. and Barbier, R. (1972). Perméabilité et ultrastructures des oeufs de deux Lépidoptères Tineidae: *Monopis rusticella* et *Trichophaga tapetzella*. *J. Insect Physiol*. **18**, 1447-1462.

Cruickshank, W. J. (1972). Ultrastructural modifications in the follicle cells and egg membranes during development of flour moth oocytes. *J. Insect Physiol*. **18**, 485-498.

Cussler, E. L. (1997). *Diffusion: Mass Transfer in Fluid Systems*, 2nd edn. Cambridge: Cambridge University Press.

Daniel, S. H. and Smith, R. H. (1994). Functional anatomy of the egg pore in *Callosobruchus maculatus*: a trade-off between gas-exchange and protective functions? *Physiol. Entomol.* **19**, 30-38.

Denny, M. W. (1993). *Air and Water*. Princeton: Princeton University Press.

Donhowe, I. G. and Fennema, O. (1993). Water vapor and oxygen permeability of wax films. *J. Am. Oil Chem. Soc.* **70**, 867-873.

Dorn, A., Bishoff, S. T. and Gilbert, L. I. (1987). An incremental analysis of the embryonic development of the tobacco hornworm, *Manduca sexta*. *Inter. J. Invert. Reprod. Develop.* **11**, 137-158.

Dudley, R. and Chai, P. (1996). Animal flight mechanics in physically variable gas mixtures. *J. Exp. Biol*. **199**, 1881-1885.

Fehrenbach, H. (1995). Egg shells of Lepidoptera – fine structure and phylogenetic implications. *Zoologischer Anzeiger* **234**, 19-41.

Fehrenbach, H., Dittrich, V and Zissler, D. (1987). Eggshell fine structure of three lepidopteran pests: *Cydia pomonella* (L.) (Torticidae), *Heliothis virescens* (Fabr.) and *Spodoptera littoralis* (Boisd.) (Noctuidae). *Inter. J. Insect Morphol. Embryol*. **16**, 201-219.

Furneaux, P. J. S. and Mackay, A. L. (1972). Crystalline protein in the chorion of insect eggshells. *J. Ultrastruct. Res.* **38**, 343-359.

Gibbs, A. G. (1998). Water-proofing properties of cuticular lipids. *Am. Zool.* **38**, 471-482.

Gibbs, A. G. (2002). Lipid melting and cuticular permeability: new insights into an old problem. *J. Insect Physiol.* **48**, 391-400.

Gilby, A. R. and Cox, M. E. (1963). The cuticular lipids of the cockroach *Periplaneta americana* (L.). *J. Insect Physiol*. **9**, 671-681.

Hartley, J. C. (1971). The respiratory system of the egg-shell of *Homorocoryphus nitidulus vicinus* (Orthoptera, Tettigoniidae). *J. Exp. Biol*. **55**, 165-176.

Hinton, H. E. (1981). *Biology of Insect Eggs*, Vol. 1. Oxford: Pergamon Press.

Lamer, A. and Dorn, A. (2001). The serosa of *Manduca sexta* (Insecta, Lepidoptera): ontogeny, secretory activity, structural changes and functional considerations. *Tissue Cell* **33**, 580-595.

Lockey, K. H. (1976). Cuticular hydrocarbons of *Locusta*, *Schistocerca* and *Periplaneta* and their role in waterproofing. *Insect Biochem*. **6**, 457-472.

Lockey, K. H. (1988). Lipids of the insect cuticle: origin, composition and function. *Comp. Biochem. Physiol. B* **89**, 595-645.

Machin, J. (1980). Cuticle water relations: towards a new cuticle waterproofing model. In *Insect Biology in the Future: 'VBW 80'* (ed M. Locke and D. S. Smith), pp. 79-105. New York: Academic Press.

Margaritis, L. H. (1985). Structure and physiology of the eggshell. In *Comprehensive Insect Physiology, Biochemistry and Pharmacology*, vol. 1 (ed. G. A. Kerkut and L. I. Gilbert), pp. 153-230. Oxford: Pergamon Press.

Margaritis, L. H., Hamodrakas, S. J., Arad, T. and Leonard, K. R. (1984). Three-dimensional reconstruction of innermost chorion layer in *Drosophila melanogaster*. *Biol. Cell* **52**, 279-284.

Margaritis, L. H., Kafatos, F. C. and Petri, W. H. (1980). The egg-shell of *Drosophila melanogaster*. Fine structure of the layers and regions of the wild-type egg-shell. *J. Cell Sci*. **43**, 1-35.

Margaritis, L. H. and Mazzini, M. (1998). Structure of the egg. In *Microscopic Anatomy of the Invertebrates*, *Insecta*, vol. 11C (ed. F. W. Harrison, M. Locke), pp. 995-1037. New York: Wiley Liss.

Margaritis, L. H., Petri, W. H. and Wyman, A. R. (1979). Structure and image analysis of a crystalline layer from Dipteran egg-shell. *Cell Biol. Int. Rep*. **3**, 61-67.

Nelson, D. R. and Sukkestad, D. R. (1970). Normal and branched aliphatic hydrocarbons from the eggs of the tobacco hornworm. *Biochemistry* **9**, 4601-4611.

Nelson, D. R. and Leopold, R. A. (2003). Composition of the surface hydrocarbons from the vitelline membranes of dipteran embryos. *Comp. Biochem. Physiol. B* **136**, 295-308.

Ocko, B. M., Wu, Z., Sirota, E. B., Sinha, S. K., Gang, O. and Deutsch, M. (1997). Surface freezing in chain molecules: Normal alkanes. *Phys. Rev. E* **55**, 3164-3182.

Orfanidou, C. C., Hamodrakas, S. J., Margaritis, L. H., Galanopoulos, V. K., Dedieu, J. C. and Gulik-Krzywicki, T. (1992). Fine structure of the chorion of *Manduca sexta* and *Sesamia nonagrioides* as revealed by scanning electron microscopy and freeze-fracturing. *Tissue Cell* **24**, 735-744.

Paganelli, C. V. (1980). The physics of gas exchange across the avian eggshell. *Am. Zool.* **20**, 329-338.

Paganelli, C. V., Ar, A., Rahn, H. and Wangensteen, O. D. (1975). Diffusion in the gas phase: the effects of ambient pressure and gas composition. *Resp. Physiol.* **25**, 247-258.

Papanikolaou, A. M., Margaritis, L. H. and Hamodrakas, S. J. (1986). Ultrastructural analysis of chorion formation in the silkmoth *Bombyx mori*. *Can. J. Zool.* **64**, 1158-1173.

Papassideri, I. S. and Margaritis, L. H. (1996). The eggshell of *Drosophila melanogaster*: IX. Synthesis and morphogenesis of the innermost chorionic layer. *Tissue Cell* **28**, 401-409.

Papassideri, I., Margaritis, L. H. and Gulik-Krzywicki, T. (1991). The egg-shell of *Drosophila melanogaster* VI. Structural analysis of the wax layer in laid eggs. *Tissue Cell* **23**, 567-575.

Papassideri, I. S., Trougakos, I. P., Leonard, K. R. and Margartis, L. H. (2003). Structure and biochemical analysis of the *Leptinotarsa decemlineata* (Coleoptera; Chrysomeloidea) crystalline chorionic layer. *J. Insect Physiol.* **49**, 377-384.

Rahn, H. and Ar, A. (1974). The avian egg: incubation time and water loss. *Condor* **76**, 147-152.

Salkeld, E. H. (1973). The chorionic architecture and shell structure of *Amathes c-nigrum* (Lepidoptera: Noctuidae). *Can. Entomol.* **105**, 1-10.

Schmidt-Nielsen, K. (1984). *Scaling: Why is Animal Size So Important?* Cambridge: Cambridge University Press.

Schreuders, P. D., Kassis, J. N., Cole, K. W., Schneider, U., Mahowald, A.

P. and Mazur, P. (1996). The kinetics of embryo drying in *Drosophila melanogaster* as a function of the steps in permeabilization: experimental. *J. Insect Physiol.* **42**, 501-516.

Slifer, E. H. (1948). Isolation of a wax-like material from the shell of the grasshopper egg. *Disc. Faraday Soc.* **3**, 182-187.

Telfer, W. H. and Smith D. S. (1970). Aspects of egg formation. *Symp. Roy. Entomol. Soc. Lond.* **5**, 117-134.

Thorpe, W. H. and Crisp, D. J. (1947). Studies on plastron respiration II. The respiratory efficiency of the plastron in *Aphelocheirus*. *J. Exp. Biol.* **24**, 270-303.

Tøien, Ø., Paganelli, C. V., Rahn, H. and Johnson, R. R. (1987). The influence of eggshell pore shape on gas diffusion. *J. Exp. Zool.* Suppl. 1, 181-186.

Tøien, Ø., Paganelli, C. V., Rahn, H. and Johnson, R. R. (1988). Diffusive resistance of avian eggshell pores. *Resp. Physiol.* **74**, 345-354.

Toolson, E. C., White, T. R. and Glaunsinger, W. S. (1979). Electron paramagnetic resonance spectroscopy of spin-labelled cuticle of *Centruroides sculpturatus* (Scorpiones: Buthidae): correlation with thermal effects on cuticular permeability. *J. Insect Physiol.* **25**, 271-275.

Tuft, P. H. (1950). The structure of the insect egg-shell in relation to the respiration of the embryo. *J. Exp. Biol.* **26**, 22-34.

Wangensteen, O. D. and Rahn, H. (1970/71). Respiratory exchange by the avian embryo. *Resp. Physiol.* **11**, 31-45.

Wangensteen, O. D., Wilson, D. and Rahn, H. (1970/71). Diffusion of gases across the shell of the hen's egg. *Resp. Physiol.* **11**, 16-30.

Woods, H. A. and Hill, R. I. (2004). Temperature-dependent oxygen limitation in insect eggs. *J. Exp. Biol.* **207**, 2267-2276.

Woods, H. A. and Singer, M. S. (2001). Contrasting responses to desiccation and starvation by eggs and neonates of two Lepidoptera. *Physiol. Biochem. Zool*. **74**, 594-606.

Appendix 1. Concentrations can be recast in terms of partial pressures by replacing ΔC with $\beta * \Delta P_{O_2}$ where β is the capacitance coefficient (= $\Delta C / \Delta P$) and P_{O_2} is the partial pressure of O_2 at the egg mass surface (Dejours 1981). Although β is, strictly, unknown for most layers, it can be approximated using published data for different classes of material—water, wax, tissue, etc.

Appendix 2. Eggs of *Manduca sexta* are oblate spheroids with two axes, an equatorial axis (a, long axis, parallel to leaf's surface) and a polar axis (c, orthogonal to leaf surface). Average values of a and c for eggs from our laboratory colony are 0.784 mm and 0.684 mm, respectively. The axis measurements can be used to calculate surface area by the formula

$$S = 2\pi a^2 + \pi \frac{c^2}{e} \ln\left(\frac{1+e}{1-e}\right),$$

where e, the ellipticity, is given by $\sqrt{1 - c^2/a^2}$. For colony eggs, the average surface area is 7.07 mm^2 (or 7.07×10^{-6} m^2). Volume is calculated as

$$V = \frac{4}{3}\pi a^2 c,$$

giving 1.76 mm^3, or 1.76×10^{-9} m^3.

The average mass of a 3-d old egg from our colony is 1.56 mg, indicating a density (mass/volume) of 0.88. And indeed, 3-d old eggs do float, even though newly deposited eggs do not, implying that volume stays more or less constant even though mass decreases over development.

Appendix 3. The trabecular layer will contain a uniform composition of gas throughout its extent if the resistance to sideways flux within the trabecular layer is much less than the resistance to radial flux across the wax layer—i.e., if:

$$\frac{l}{D_2} << \frac{d_3 H_3}{D_3}$$

where l is the average distance between aeropyles. Orfanidou et al. (1992) estimate that aeropyles of *M. sexta* are about 30 μm (= 3 x 10^{-5} m) apart, and our data show that they are somewhat further apart. Using Orfanidou et al.'s data,

$$\frac{l}{D_2} = 3 \text{ x } 10^{-5} \text{ m} / \ 2.61 \text{ x } 10^{-6} \text{ m}^2 \text{ s}^{-1} \ = \ 11.5 \text{ s m}^{-1}.$$

In the main body of the paper we estimate:

$$\frac{d_3 H_3}{D_3} = 4.7 \text{ x } 10^6 \text{ s m}^{-1}.$$

Thus, the resistance of the trabecular layer is five orders of magnitude smaller than that in the wax, meaning that the gas layer in it is everywhere uniform.